

# Multifractal Analysis of Medical Images

Andrea Silveti and Claudio Delrieux

Departamento de Ingeniería Eléctrica y de Computadoras  
Instituto de Investigaciones en Ingeniería Eléctrica - IIIE (UNS-CONICET)  
Universidad Nacional del Sur — Alem 1253 - Bahía Blanca - Argentina  
claudio@acm.org (Partially funded by SECyT-UNS)

**Abstract:** Automatic segmentation of different types of tissue from medical images of several sensing modalities is of great importance for clinical and research applications. In this paper, we propose a segmentation methodology based on a multifractal approach. We present different alternatives for estimating local fractal exponents in these images, as well as their global distributions—the multifractal spectrum. We generate new images by means of grayscale mapping of these local and global computed values. The obtained results are quite promising as a tissue differentiation tool, and therefore are suitable to carry out automatic segmentation of abnormalities in medical images.

**Keywords:** Medical Imaging — Image Segmentation — Hölder Exponent — Multifractals

## 1 Medical Image Segmentation

Medical images are becoming the mainstream procedure in many medical practices like diagnosis, surgery planning, radiotherapy, anomalous tissue detection, among many other. Image acquisition methods comprehend several modalities including computed tomography (CT), magnetic resonance (MRI), functional magnetic resonance (fMRI), single positron emission computed tomography (SPECT), positron emission tomography (PET) [16,8]. Image segmentation is one of the most important and challenging topic within medical image processing. It consists in getting a specific description of an entity in terms of contours or regions. For this purpose, the identification of contours or regions with similar descriptive features is needed to detect boundaries, or to facilitate region separation in a precise manner.

Traditional segmentation methods, based on differential operators, turn out to be unsatisfactory, particularly in assisted medical diagnosis applications, given that most medical imaging modalities are prone to noise and other sensing fluctuations that are amplified by the differential operators [2,5]. For this reason, and taking into account that human tissue is characterized by a high degree of self-similarity, fractal descriptors turn out to be more suitable image descriptors for boundary segmentation than local differential properties [6,11,10].

Local fractal dimension is a distinguishing characteristic in pathological tissues classification process [3,4]. The regularity differences between regions, borders or isolated points with respect to the background allow to discriminate among structures –however irregular they seem to be. Whenever these structures are not identified from an anatomical point of view, it is possible to assume them as deviations of a global regularity of some kind of tissue, and therefore, as an anomaly that triggers a further, supervised, analysis.

Multifractal theory applied to 2D and 3D medical images is based on analysing the local behavior in the limit of a measure, computed in every point of the image [7]. Subsequent global analysis of these local behaviors allows to recognize, classify, and extract both geometric or statistic distinctive features of the image. In this sense, it is possible to segment different areas of the image by means of several criteria combination, which simultaneously takes into account the local distribution of the measure (texture) with the global structure of the area to be segmented (form) [15].

## 2 Multifractal Analysis

Many natural objects and phenomena exhibit self-similar or fractal properties. In this sense, they are made of small parts exactly or statistically self-similar and scale-invariant. The fractal dimension FD, is an exponent that relates the self affine invariance or statistically self similarity in the presence of scale changes [6,9]. Deterministic fractals are characterized by the same FD in all scales, i.e. their structure is exactly self-similar and consequently are coined as “monofractals” (e.g. Cantor Set, Koch curve). On the other hand, random fractals are characterized by a set of FD which varies with the observed scale, i.e. their structures are statistical self-similar and consequently are multifractals. This is the case of natural fractals whose structures are assumed as made of many fractal subsets with different scaling behavior coexisting simultaneously [1].

### 2.1 Hölder Exponent and Hausdorff Dimension

Informally, the usual way to proceed in multifractal analysis is examining the local behavior in the limit of a measure  $\mu$  at every point of the set, i.e. finding the Hölder exponent  $\alpha$  describing the pointwise singularity index of the set, and deriving the multifractal spectrum  $f(\alpha)$  indicating the distribution of the singularities indexes  $\alpha$  along the image.

Let  $E$  be a structure divided into nonoverlapping boxes  $E_i$  of size  $\epsilon$  such that  $E = \cup_i E_i$ . Each box  $E_i$  is characterized by a measurement  $\mu(E_i)$ . From the multifractal analysis point of view, is better to express this value as a function of the scale, i.e. relative to the box size, and therefore

$$\alpha_i = \frac{\ln(\mu(E_i))}{\ln(\epsilon)}, \quad (1)$$

when  $\epsilon$  tends to zero,  $E_i$  tends to a point of the structure, so the Hölder Exponent of this point is defined as the limiting value

$$\alpha = \lim_{\epsilon \rightarrow 0}(\alpha_i). \quad (2)$$

The  $\alpha$  exponent evaluated in a point  $E$  of the structure, locally characterize its regularity. Now we need to describe the global regularity of the structure, so we must find the distribution of  $\alpha$  within  $E$ . This step consists in finding the  $f(\alpha_i)$  relating the the number of boxes of size  $\epsilon$  characterized by  $\alpha_i$ , with the box size

$$f_\epsilon(\alpha_i) = -\frac{\ln(N_\epsilon(\alpha_i))}{\ln(\epsilon)}, \quad (3)$$

When  $\epsilon$  tends to zero, the limiting value is the fractal dimension of the subsets of  $E$  characterized by  $\alpha$  –the Hausdorff Dimension of the  $\alpha$  distribution–, also known as the *multifractal spectrum*  $f(\alpha)$ .

$$f(\alpha) = \lim_{\epsilon \rightarrow 0}(f_\epsilon(\alpha)). \quad (4)$$

## 2.2 Multifractal Image Analysis

The input of the developed algorithms is restricted to 2D grayscale digital images of size  $n \times n$  with  $n = 2^k$  and  $k > 0$ . Computing the Hölder exponent in a pixel  $(x,y)$  of the image (Eq. 2) implies the use of linear regression to fit a straight line to the paired data  $(\log(\epsilon), (\log(\mu(E_i))))$ , for  $\epsilon = 2^{i+1}$  with  $i \geq 0$ , and subsets  $E_i$  corresponding to boxes of sizes  $\epsilon \times \epsilon$  centered in  $(x,y)$ . The slope of this regression line is the Hölder exponent related to the pixel.

Based on this exponents is posible to generate an  $\alpha$ -image with the same size of the original image, setting each pixel  $(x,y)$  of the new one with a gray-scale mapping of the Hölder exponent  $\alpha$  computed for  $(x,y)$  in the original one.

For simplicity, Box dimension [9] is used to comput the Hausdorff dimension defined in Eq. 4. Computing this dimension for a particular Hölder exponent  $\alpha$  is the same as computing the Box dimension of a binary image resulting from thresholding the  $\alpha$ -image with *threshold* =  $\alpha$ . However, since the Hölder exponent is a noninteger value, and theoretically is posible to have  $n \times n$  different values in the image, we must set up a number  $C$  of equivalence classes of  $\alpha$ -values and consequently compute the multifractal spectrum only for these values.

Let  $\alpha_{min}$  and  $\alpha_{max}$  be the minimum and maximum Hölder exponent of the image, we obtain  $C$  values  $\alpha_c = \alpha_{min} + (c - 1)((\alpha_{max} - \alpha_{min})/C)$  within the interval  $[\alpha_{min}.. \alpha_{max})$ . Then,  $\alpha$  belong to the  $\alpha_c$  equivalence class, for  $c = 1, 2, \dots, C$ , if  $\alpha_c \leq \alpha < \alpha_{c+1}$ . The particular case  $\alpha = \alpha_{max}$  belong to  $\alpha_C$ . Finally, we obtain the slope of the correlation between  $N_\epsilon(\alpha_c)$  and  $\epsilon$  in log—log space, again with  $\epsilon = 2i + 1$  con  $i \geq 0$ . This slope is the value of  $f(\alpha_c)$ , and must be computed for  $c = 1, 2, \dots, C$  in order to generate an  $f(\alpha)$ -image of size  $n \times n$  quantized with only  $C$  different intensity values, —one for each  $f(\alpha_c)$ . This image is such that all pixels of the original one, with Hölder exponent belonging to the  $\alpha_c$  equivalence class, will get the same intensity value corresponding to  $f(\alpha_c)$ .

### 2.3 Multifractal Measures

Informally it was said that multifractal theory applied to images, analyze the local behavior in the limit of a measure  $\mu$  in every point of the set. Different measures lead to different Hölder exponents, and consequently to different global regularity indicators of the set and different global distributions of the regularity. This means that according to the information required to extract from the image, several alternatives are proposed. In this work, different kind of measures were implemented: capacity measures —maximum, minimum, sum, iso measure— (the most frequently used), and differential measures of capacity —absolute difference, central absolute difference— (which coincide with quadratic and lineal self correlation exponents [13,12,14]). In all the cases, measures are defined as a function of the gray level of the point belonging to the region.

Let  $(x, y)$  be a pixel of the original image,  $Image(i, j)$  be the gray level (intensity) of the pixel  $(i, j)$ ,  $t$  be the size of the measure domain centered in  $(x, y)$ ,  $\Omega$  be the set of pixels  $(i, j)$  within the image domain,  $\Omega^*$  be the set of pixels  $(i, j)$  with nonzero intensity within the image domain; the following measures  $\mu_t(x, y)$  are defined:

$$Max_t(x, y) = \max_{(i,j) \in \Omega} Image(i, j), \quad (5)$$

$$Min_t(x, y) = \min_{(i,j) \in \Omega^*} Image(i, j), \quad (6)$$

$$Iso_t(x, y) = cardinality\{(i, j) \mid Image(x, y) \equiv Image(i, j), (i, j) \in \Omega\}, \quad (7)$$

$$Sum_t(x, y) = \sum_{(i,j) \in \Omega} Image(i, j), \quad (8)$$

$$DifAbs_t(x, y) = \max_{(i,j),(k,l) \in \Omega} | Image(i, j) - Image(k, l) |, \quad (9)$$

$$DifAbsCentral_t(x, y) = \max_{(i,j) \in \Omega} | Image(x, y) - Image(i, j) |. \quad (10)$$

This leads to the possibility to explore a range of characteristic descriptors associated to images, adapting the multifractal segmentation to the particular

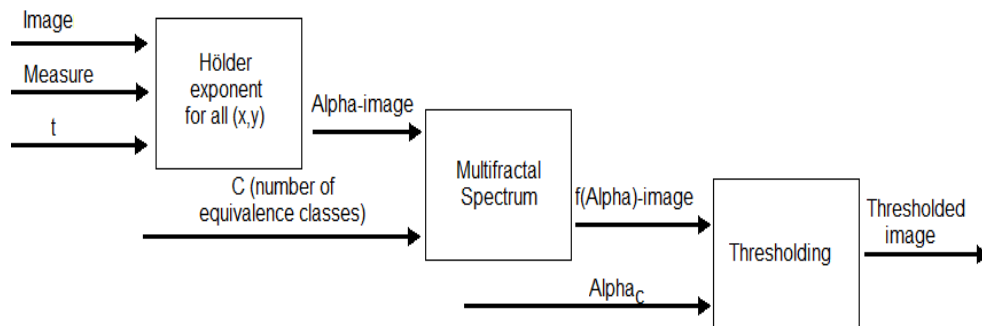


**Fig. 1.** Processing Pipeline

application. Fig. 1 shows the processing pipeline resulting from the segmentation methodology.

### 3 Results

Fig. 2 show the user interface of the system developed for testing the methodology. In the processed example, four images are shown, the original image to be processed, the  $\alpha$ -image resulting from the application of the local Hölder exponent, the  $f\alpha$ -image corresponding to the multifractal spectrum, and a binary image obtained by thresholding the  $\alpha$ -image for a particular multifractal spectrum interval. The bottom part of the interface shows the multifractal spectrum over which the user can choose the meaningful range of values from a statistic point of view. The top part, shows the dropdown menu bar that includes all the options implemented.

This particular example image come from a digital mammogram. The early detection of breast cancer greatly improves prognosis. One of the first signs of cancer is the formation of clusters of microcalcifications, so an important goal of this kind of image processing is precisely the early detection of microcalcifications, as well as comparison and monitoring of pathological tissues evolution.

Another example of multifractal processing was applied to a slice of a Computed Tomography (Fig. 3). Systematic processing of all slices can derive in automatic segmentation of different types of tissue.

### 4 Conclusion and Further Work

In this work we presented the development of an image processing system based on multifractal theory, which is mainly oriented to medical image processing.

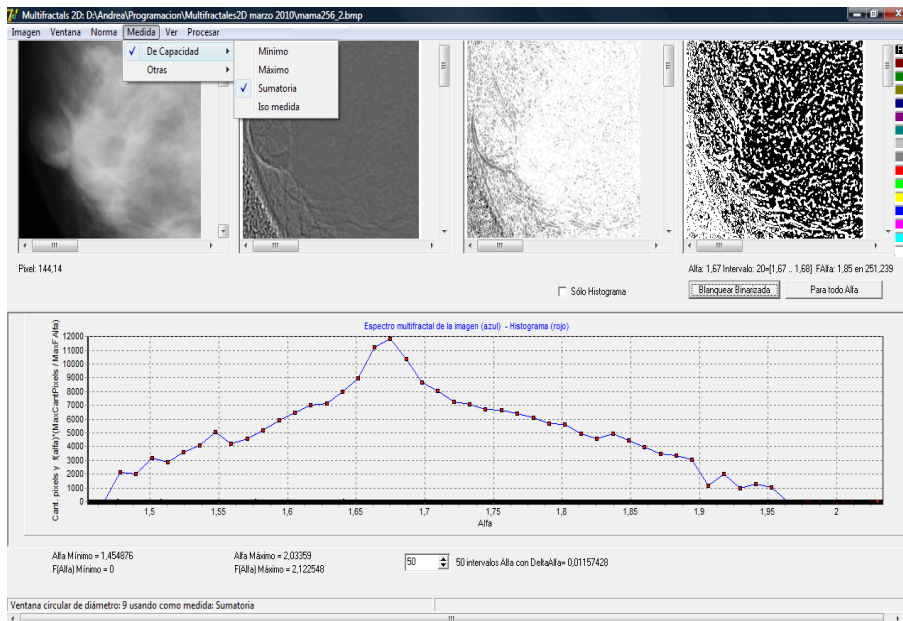


**Fig. 2.** User Interface of the developed system.

We introduced the mathematical background concerning multifractal measures, the numerical evaluation techniques, and the associated methodologies. These concepts were implemented in a processing tool, and some preliminary results applying multifractal theory to medical images (mammograms and CT) were shown. We are currently validating the accuracy of the processing tool with theoretical fractal sets whose multifractal spectrum can be mathematically known, as well as applying the results in 3D image modalities to achieve full 3D image segmentation.

## References

1. C. Evertsz and B. Mandelbrot. Multifractal Measures. In P. Andrews H. Peitgen, H. Jurgens, editor, *Chaos and Fractals*. Springer, Amsterdam, 1992.
2. Rafael González and Richard Woods. *Digital Image Processing*. Addison-Wesley, Wilmington, USA, 1996.
3. Pascal Mignot Jacques Levy-Vehel and Jean-Paul Berror. Multifractal, texture, and Image analysis. In *Conference on Computer Vision and Pattern Recognition*, pages 661–664. IEEE, 1992.
4. Jacques Levy-Vehel and Robert Vojak. Multifractal analysis of Choquet capacities. *Advances in applied mathematics*, 20(1):1–43, 1998.
5. Jae Lin. *2D Signal and Image Processing*. Prentice-Hall, Cambridge, 1991.
6. B. Mandelbrot. *The Fractal Geometry of Nature*. W. H. Freeman, New York, 1983.

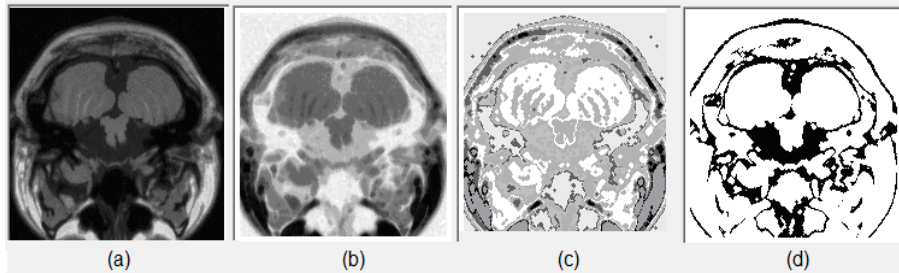


**Fig. 3.** Processing example of a CT image: ( a) Original Image, ( b)  $\alpha$ -image, ( c)  $f\alpha$ -image, ( d) binary image for a multifractal spectrum interval.

7. Ethel Nilsson. Multifractal-based image analysis with applications in medical imaging. Technical Report Masters Thesis in Computing Science and Mathematics, Umea University, Sweden, 2007.
8. Yamashiro P. Fractal Analysis of MRI. Technical Report Medical Sciences Lab., University of Washington, Seattle, 1997.
9. H.-O. Peitgen and D. Saupe. *The Science of Fractal Images*. Springer-Verlag, New York, 1986.
10. Irine S. Reljin and Branimir D. Reljin. Fractal geometry and Multifractals in analyzing and rocessing medical data and images. *Archive of Oncology*, 10(4):283–293, 2002.
11. Irine S. Reljin, Branimir D. Reljin, Ivan Pavlovic, and Ivana Rakocevic. Multifractal analysis of gray-scale images. *MEleCon*, pages 490–493, 2000.
12. A. Silveti and C. Delrieux. Dimensión Fractal de Autocorrelación Cuadrática en Imágenes Digitales. In *XII Congreso Argentino de Ciencias de la Computación, Corrietes y Resistencia*, Argentina, 2007. CACIC, .
13. A. Silveti and C. Delrieux. Medición de la Dimensión Fractal en Superficies. In *Workshop de Investigadores en Ciencias de la Computación*, pages 81–85, Trelew, Argentina, 2007. WICC, .
14. A. Silveti and C. Delrieux. Un Método Robusto para Evaluar Dimensión Fractal Local en Imágenes. In *XII Reunión de Trabajo en Procesamiento de la Información y Control*, Río Gallegos, Argentina, 2007. RPIC, .
15. Tatijana Stojic and Borko Stojic. Multifractal Analysis of Human Retinal Vessels. *IEEE Transactions on Medical Imaging*, 25(8):259–270, 2006.
16. Cai W., Walter S., and Karangelis G.and Sakas G. Collaborative virtual simulation environment for radiotherapy treatment planning. *Computer Graphics Forum*, 19:379–390(12), September 2000.